HII Regions in M33: Spectral Parameters Variations & 2D IFU Spectroscopy

José M. Vílchez

I.A.A. – CSIC (Granada, SPAIN)

Arcetri, Firenze Sept 2009

Monica Relaño
Ana Monreal
Enrique Perez Montero
Angeles Diaz

as well as

F. Bresolin , Jesus Lopez
R. Kennicutt, G. Stasinska
E. & R. Terlevich …

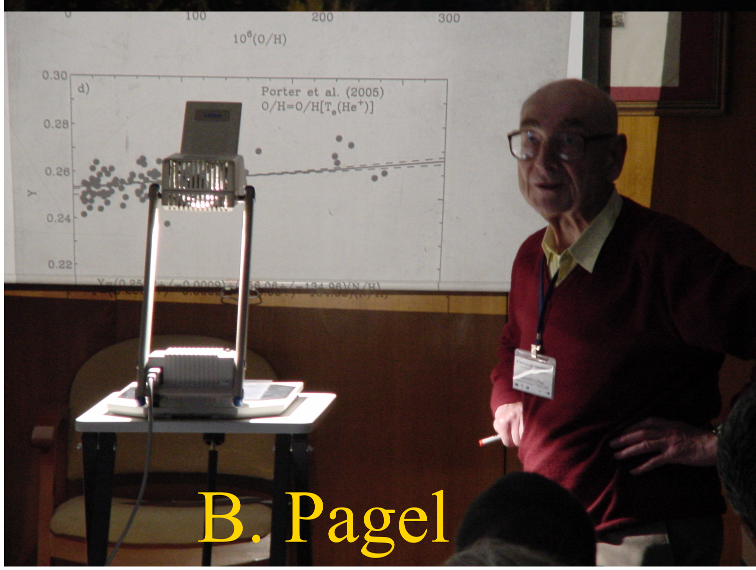

Active star formation in the triangulum galaxy

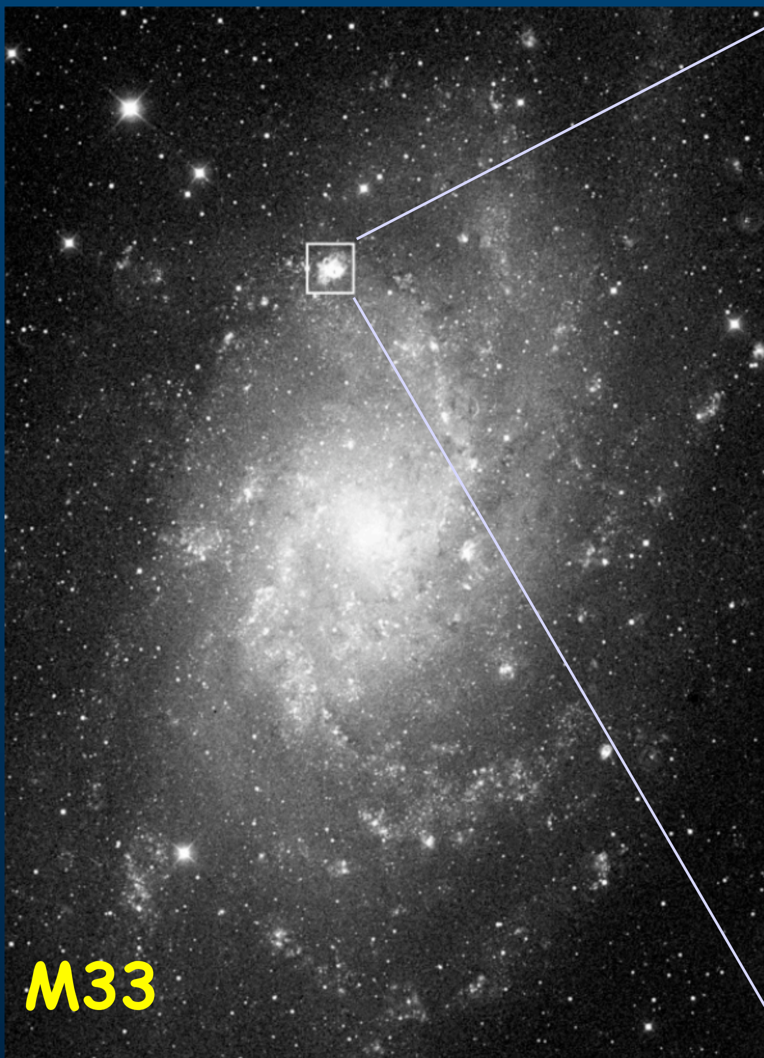

M33 in the Local Group: northern HII regions best examples

M33 offers a unique opportunity in order to perform detailed studies of the physics of extragalactic star formation regions with the necessary spatial resolution.

Motivation. Extragalactic HII regions provide info on chemistry & massive stars: BUT their study =>

a multi spatial-scale problem

Galactic nebula @ small scale (~10^{-2} few pc)
Giant extrag. HII R @ large scale (across discs ~ Kpc) Distant star-forming galaxies @ entire galaxy scale

M33 helps to understand the mechanisms driving massive star formation & chemical evolution in distant galaxies

Pioneering Observations of *Extragalactic* Emission-line Regions

THE SPECTRA OF THE EMISSION NEBULOSITIES IN MESSIER 33

LAWRENCE H. ALLER[1]

ABSTRACT

The emission nebulosities in Messier 33 are similar in spectral characteristics to those of our own Galaxy and to the low-excitation planetary IC 418. The ratio of λ 5007/λ 3727 is found to be the most reliable excitation criterion for these nebulosities. The available evidence suggests that in most of these nebulosities the oxygen is predominantly in the singly ionized condition.

Astronomers have for some time recognized the presence of bright-line nebulosities in external galaxies. Seyfert[2] discovered emission nebulosities in M 101; Babcock[3] found faint emission patches at a considerable distance from the nucleus of the Andromeda nebula; while Mayall[4] has recently given a comprehensive survey of the occurrence of λ 3727 of [*O* II], and other lines as well, in the spectra of extragalactic nebulae.

Bright lines in the nebulous condensations of Messier 33 (NGC 604, 588, and 595) have been observed by Slipher,[5] by Pease,[6] and by Hubble.[7] A preliminary list of the emission patches observed in the rotational study of this spiral has been given elsewhere.[8] However, a more detailed and complete description of these emission nebulosities with respect to their excitation characteristics seems worth while. Accordingly, rough intensity estimates of the bright lines have been made whenever practicable.

The small dispersion of the spectrograms and the graininess of the fast emulsion used rendered impracticable the ordinary methods of spectrophotometry. Intensities, estimated with the aid of scale plates, seemed the best solution of the problem. Dr. Mayall and the writer made the scale plates in the following fashion.

While the spectrograph was off the telescope, we mounted an iris diaphragm between the spark and the slit. By varying the apertures of the iris diaphragm, which had been calibrated with a photoelectric cell in the laboratory,[9] we were able to make a series of exposures upon each type of emulsion with a fixed exposure time and with known intensity ratios. We developed the scale plates in the same way as the nebular plates. We then estimated the relative intensities of the lines in the nebular spectrum simply by comparing them with the lines on the scale plate.

Line intensities measured in this way, although better than estimates made on an arbitrary scale, may be affected by large systematic errors. The individual exposures were one second on the scale plates and several hours on the nebular spectra. The density-intensity curves derived from the former may not, therefore, be quite valid for the latter. More serious is the circumstance that the continuous background is often quite strong, and the scale-plate method makes no allowance for emission lines superposed on

[1] Society of Fellows, Harvard University.

[2] *Ap. J.*, **91**, 261, 1940.

[3] *Lick Obs. Bull.*, **19**, 41, 1939 (No. 498).

[4] *Lick Obs. Bull.*, **19**, 33, 1939 (No. 497).

[5] *Pop. Astr.*, **23**, 23, 1915; *Proc. Amer. Phil. Soc.*, **56**, 406, 1917.

[6] *Pub. A.S.P.*, **27**, 239, 1915.

[7] *Ap. J.*, **63**, 236, 1926; *Mt. W. Contr.*, No. 310.

[8] *Pub. A.S.P.*, **51**, 113, 1939.

[9] We are indebted to Dr. G. E. Kron for helping with this calibration.

Aller 1942 !! : spectra of HII regions in M33

THE ASTROPHYSICAL JOURNAL, **199**: 591–610, 1975 August 1

SPECTROPHOTOMETRIC OBSERVATIONS OF IONIZED HYDROGEN REGIONS IN NEARBY SPIRAL AND IRREGULAR GALAXIES

HARDING E. SMITH*
Astronomy Department, University of California, Berkeley
Received 1974 November 18; revised 1975 February 6

ABSTRACT

A program of direct photography and spectrophotometry has been carried out on H II regions in a selection of nearby spiral and irregular galaxies. Abundance analyses for H II regions in M101 and M33 show a strong radial gradient in the O/H ratio, decreasing by approximately a factor of 10 across the galaxy disks. The Ne/O and S/O abundance ratios are constant. The derived nitrogen abundances, coupled with the line ratios for other H II regions, indicate a weak gradient in the ratio of N/O, decreasing by about a factor of 4 from the nuclear regions outward. No large helium abundance differences are observed, although the most oxygen-poor regions may show marginally significant helium deficiencies. Excitation differences among the H II regions of Sbc–Scd–Irr galaxies can best be understood in terms of an abundance sequence which progresses from higher to lower heavy-element enrichment as one progresses from the earlier to later type galaxies.

Subject headings: abundances, nebular — galaxies — nebulae

I. INTRODUCTION

The ionized hydrogen regions that define the arms of late type spiral galaxies have an emission-line spectrum that is a one parameter sequence, characterized by the "excitation," defined as the logarithmic ratio of [O III] λλ4959, 5007 to Hβ. The excitation is in turn related to the radial distance of the H II region from the galaxy nucleus, in the sense that the forbidden oxygen lines are stronger in regions farther from the galaxy center. This effect was first noted by Aller (1942) for the H II regions in M33. Other line intensity ratios vary with radial distance as well; Burbidge and Burbidge (1962) showed that the ratio of [N II] λλ6548, 6583 to Hα is much larger near the nuclei of spiral galaxies than in the outer galaxy disks. Using a simple H II region model, Searle (1971) has explained these emission-line gradients by a general abundance gradient across the galaxy disks. Searle requires a decrease in the abundance of oxygen relative to hydrogen of about a factor of 2, and in nitrogen relative to oxygen of a factor of 10, from the nuclear regions to the outer disks in M33 and M101 in order to explain the observed differences in the spectra of these regions.

In this paper we present the results of a detailed photographic and spectrophotometric study of H II regions in nearby spiral and irregular galaxies in an attempt to sort out the effects of abundances, effective temperature of ionizing radiation, and dust content as factors determining the spectral properties of these H II regions. We believe that we are dealing with a homogeneous group of objects; they are all large ($d \geqslant 50$ pc), low-density regions ($n_e \leqslant 500\ \mathrm{cm}^{-3}$ from forbidden line ratios of Searle 1971, Comte and Monnet 1974, and this work) which must be ionized by large associations of O and B stars. This is in contrast to the more familiar nearby H II regions such as the Orion Nebula, M42. Orion is much smaller: even including the outer, low surface brightness regions, it would be barely resolved at the distance of M33, and the electron densities for the highest surface brightness regions are greater than $10^4\ \mathrm{cm}^{-3}$.

We have determined abundances of oxygen, nitrogen, neon, sulfur, and helium for nine H II regions in M101, M33, and NGC 6822. These calculated abundances provide a framework within which the emission-line intensities of a larger sample of H II regions may be understood. Our results qualitatively confirm the conclusions of Searle, showing, however, a steeper gradient in O/H and a consequently smaller N/O gradient across these galaxy disks. In the final sections we discuss the implications of our conclusions with respect to our current understanding of the production of the heavy elements and the evolution of galaxies.

II. DIRECT PHOTOGRAPHY

A program of direct interference filter photography was carried out in 1973 March and April, using the Kitt Peak National Observatory No. 1 36-inch (92 cm) telescope with a 90 mm ITT single-stage, magnetically focused image tube at the f/7.5 focus. Each galaxy was photographed through three filters: 50 Å bandpass (FWHM) interference filters centered at Hβ and λ5007 of [O III], as well as a broad-band blue filter (Corning CS-57 + Schott GG 385) covering the wavelength

* Visiting Astronomer, Kitt Peak National Observatory, which is operated by the Association of Universities for Research in Astronomy, Inc., under contract with the National Science Foundation.

e.g. ***Smith 1975****: dealed with* ***emission-line gradients*** *…*
and few others …

Methodology tests: state of the art

*>>> Standard **direct abundance derivation in HII regions:**

Tests Needed: Tests of the 2D ionisation structure

- **Chemical in-homogeneities ?**

Tests needed: 2D Study chemical enrichment/**mixing**

- **Electron Temperature fluctuations ?** (Peimbert'67)

Tests needed: **Internal T_e gradients** in HII regions

*>>> **Geometry: 3D HII regions** (Ercolano, B. et al 07)

Tests needed: chem. parameters & massive stars **in** 2D

*>>> **Ionising Clusters**. Dependence on metallicity, masses?

Tests: Galaxy gradients of **radiation hardening**

>>> (Hydro)-**Dynamical effects on** radial abundance **gradients** !! ... Tests: 2D chemical galaxy maps.

Gradients of ionising star temperatures in HII Reg

M33 shows one of the steepest radial gradients in the hardening of ionising radiation of massive star clusters .

This fact suggest a strong gradient of massive star temperatures which are higher towards larger galactic radii.

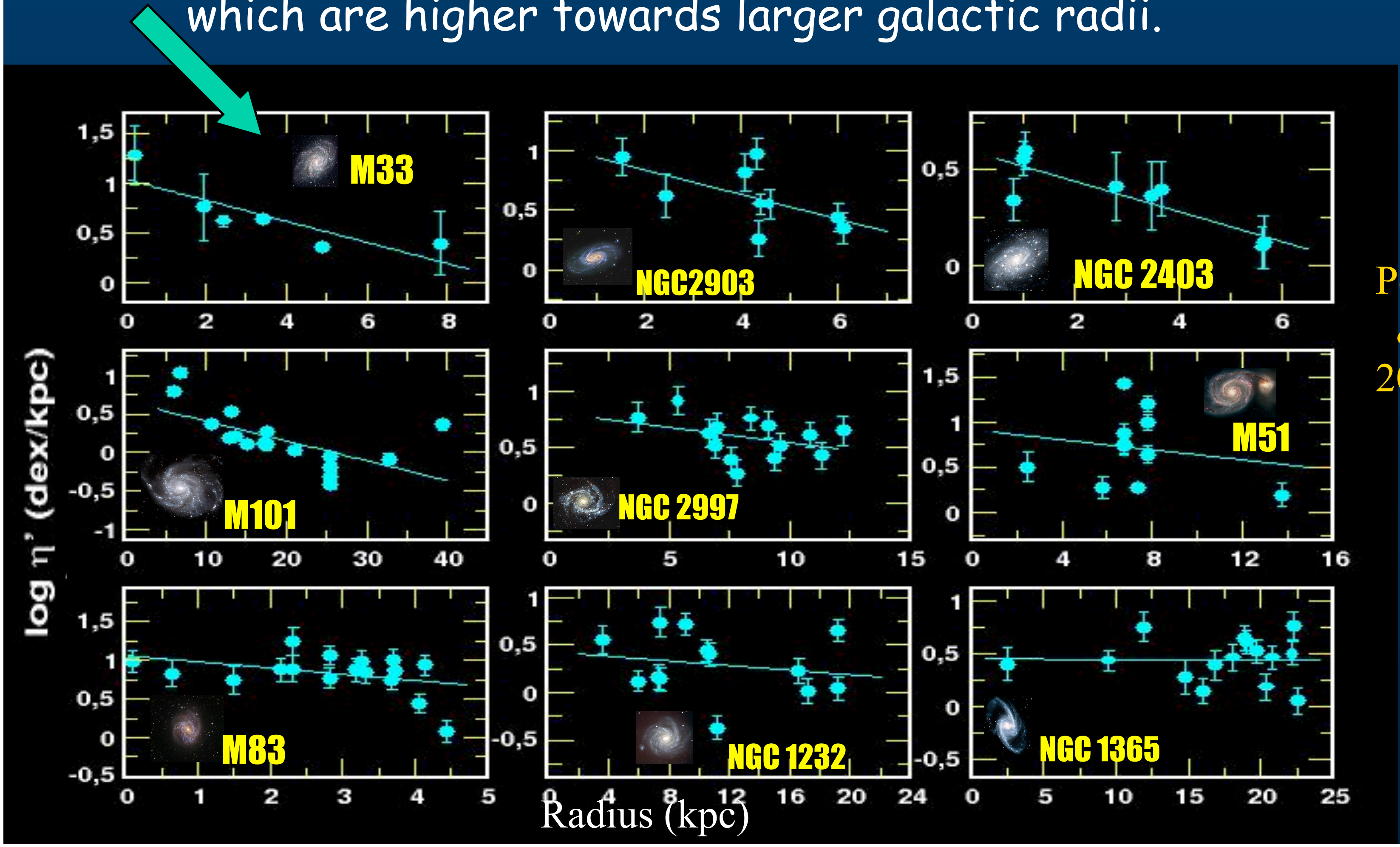

Perez-Montero & Vilchez 2009 MNRAS in press

Vilchez & Pagel (1988)

Gradients of ionising stellar temperatures of HII Regions across spiral disks

Radiation softness parameter η

region spectrum, an optical "radiation softness" parameter was defined as:

$$\eta = \frac{O^{+}/O^{2+}}{S^{+}/S^{2+}} \quad (2)$$

which does not show a strong dependence on the electron temperature and it is proportional to the corresponding ratio based on the emission lines,

$$\eta' = \frac{I([O\,\textrm{II}]\lambda 3727)/I([O\,\textrm{III}]\lambda\lambda 4959,5007)}{I([S\,\textrm{II}]\lambda\lambda 6717,6731)/I([S\,\textrm{III}]\lambda\lambda 9069,9532)} \quad (3)$$

Is a function of the stellar eff. temperature

once a given family of model atmospheres is assumed

(parameter defined by Vilchez & Pagel 1988)

Gradients of ionising star temperatures in HII Reg

M33 shows one of the steepest radial gradients in the hardening of ionising radiation of massive star clusters .

This fact suggest a strong gradient of massive star temperatures which are higher towards larger galactic radii.

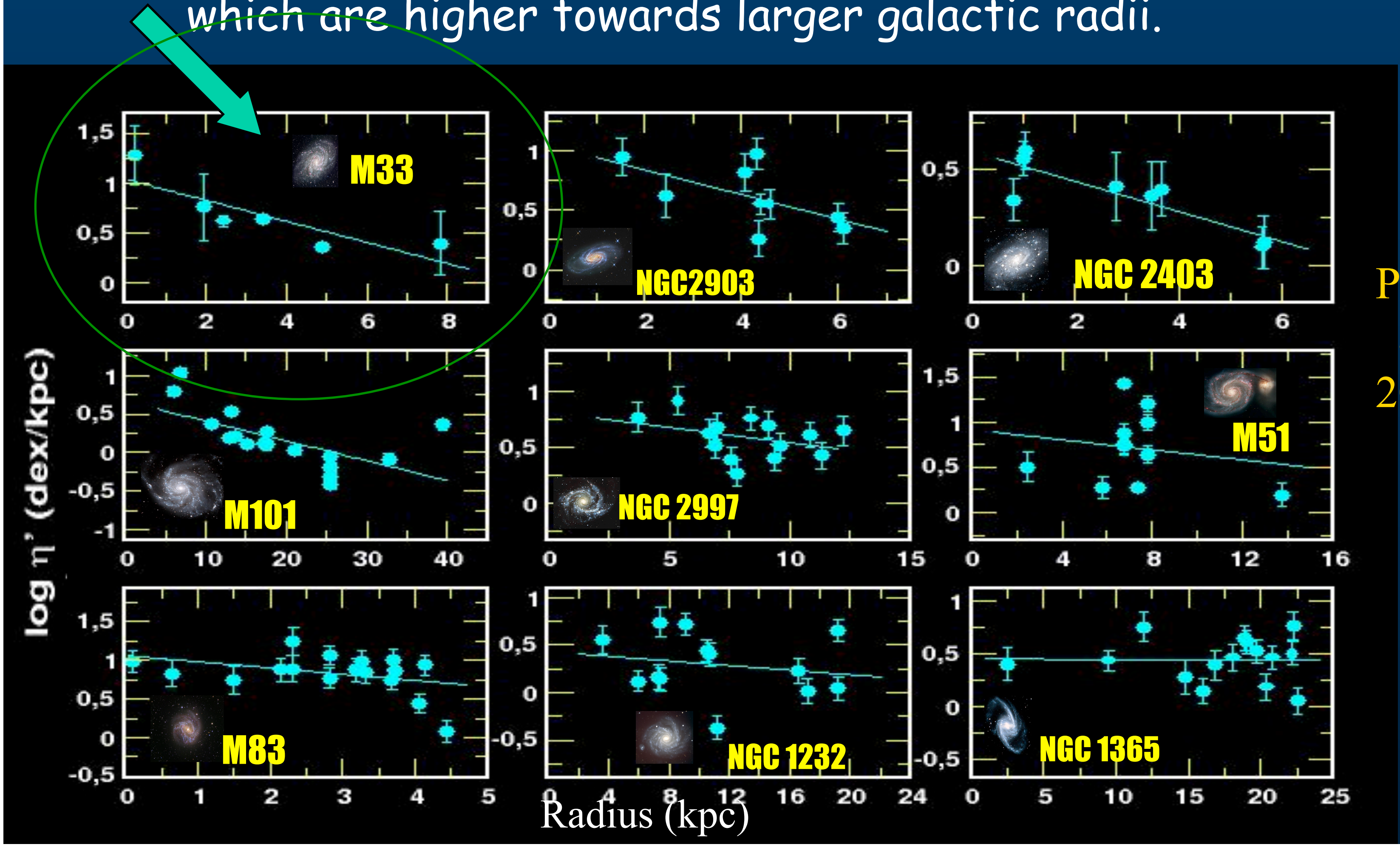

Perez-Montero & Vilchez 2009 MNRAS in press

Vilchez & Pagel (1988)

Gradients of ionising temperature of massive star clusters in HII regions

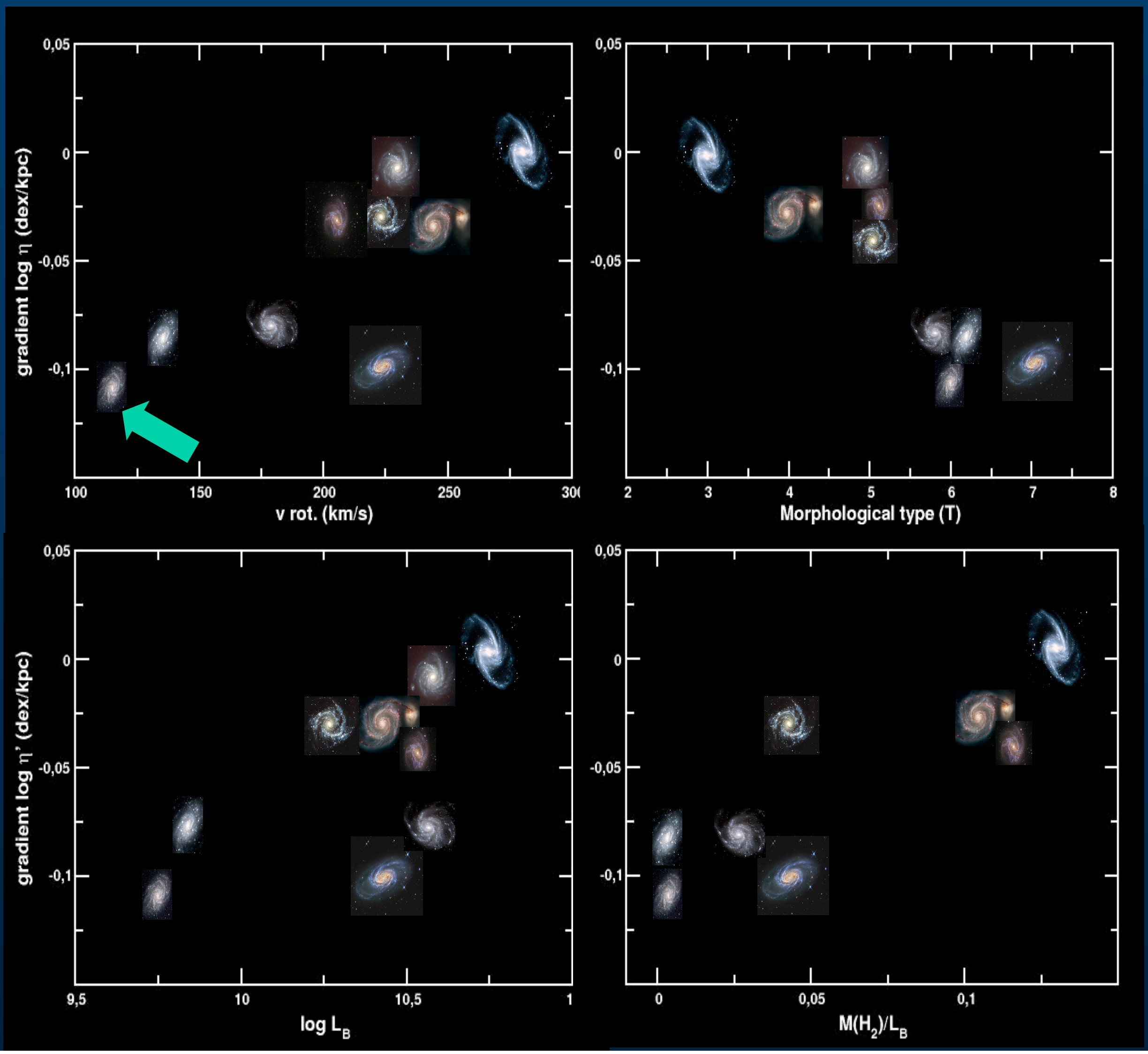

Metallicity is not the main driver of the change in the star clusters temperature:

It is suggested a star formation modulated across disks showing correlations of the gradient of T_* with:

morphological T
Galaxy Mass
Mass(H_2) /L_B

Perez-Montero & Vilchez (2009)

M33 Giant HII regions: Center, NGC 595 & IC 132

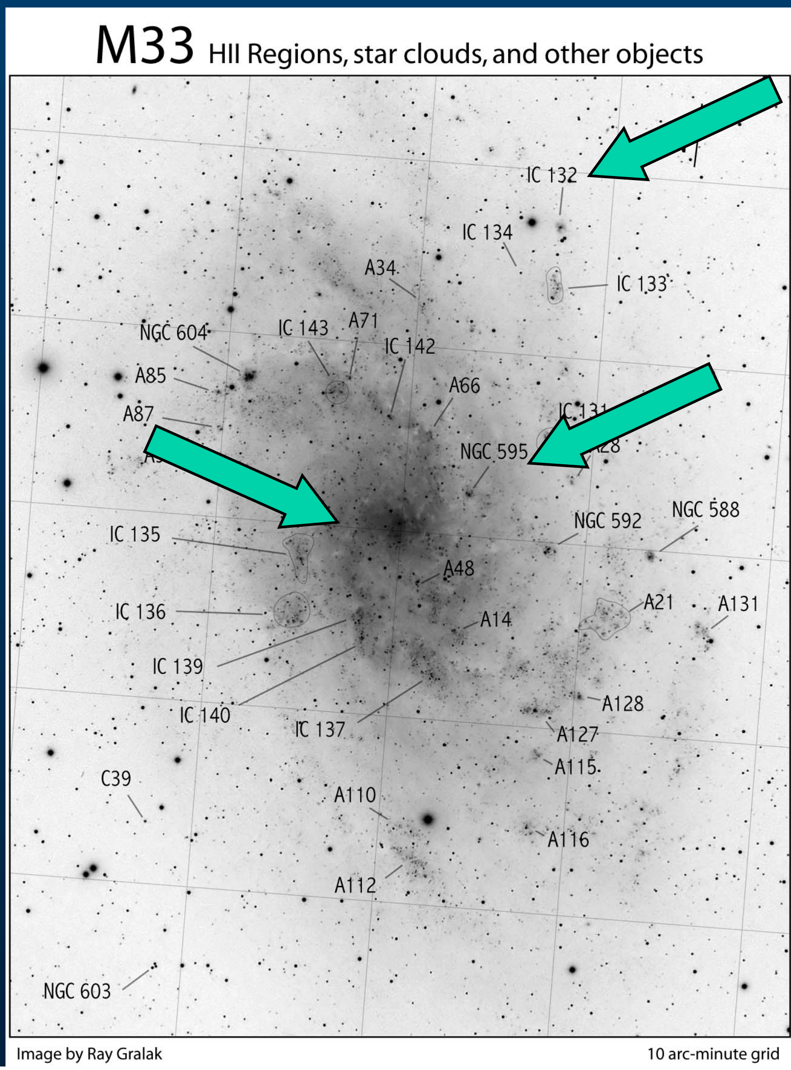

1988

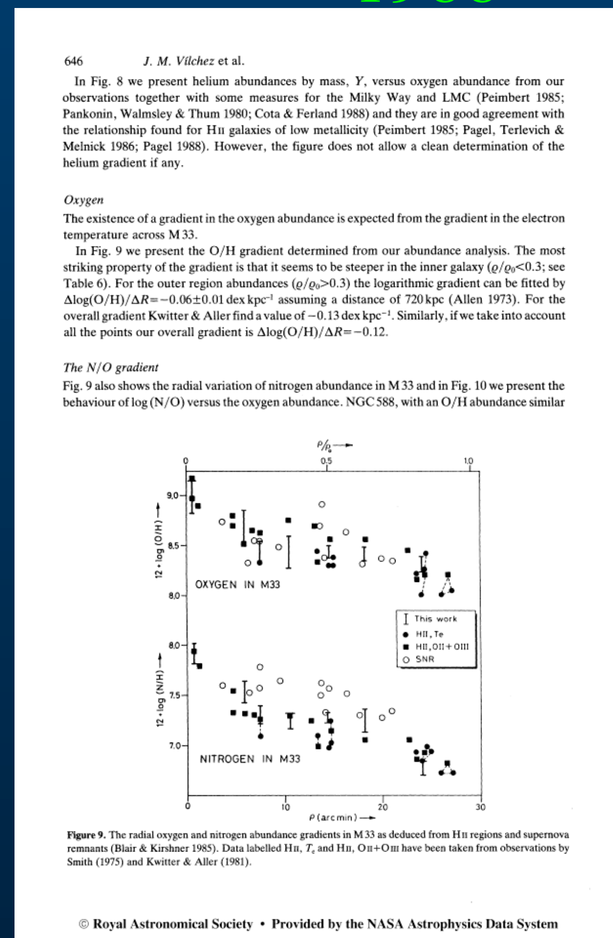

646 *J. M. Vílchez* et al.

In Fig. 8 we present helium abundances by mass, Y, versus oxygen abundance from our observations together with some measures for the Milky Way and LMC (Peimbert 1985; Pankonin, Walmsley & Thum 1980; Cota & Ferland 1988) and they are in good agreement with the relationship found for H II galaxies of low metallicity (Peimbert 1985; Pagel, Terlevich & Melnick 1986; Pagel 1988). However, the figure does not allow a clean determination of the helium gradient if any.

Oxygen

The existence of a gradient in the oxygen abundance is expected from the gradient in the electron temperature across M 33.

In Fig. 9 we present the O/H gradient determined from our abundance analysis. The most striking property of the gradient is that it seems to be steeper in the inner galaxy ($\varrho/\varrho_0<0.3$; see Table 6). For the outer region abundances ($\varrho/\varrho_0>0.3$) the logarithmic gradient can be fitted by $\Delta\log(O/H)/\Delta R=-0.06\pm0.01$ dex kpc^{-1} assuming a distance of 720 kpc (Allen 1973). For the overall gradient Kwitter & Aller find a value of -0.13 dex kpc^{-1}. Similarly, if we take into account all the points our overall gradient is $\Delta\log(O/H)/\Delta R=-0.12$.

The N/O gradient

Fig. 9 also shows the radial variation of nitrogen abundance in M 33 and in Fig. 10 we present the behaviour of log (N/O) versus the oxygen abundance. NGC 588, with an O/H abundance similar

Figure 9. The radial oxygen and nitrogen abundance gradients in M 33 as deduced from H II regions and supernova remnants (Blair & Kirshner 1985). Data labelled H II, T_e and H II, O II+O III have been taken from observations by Smith (1975) and Kwitter & Aller (1981).

PPAK Observations of the central HII regions of M33

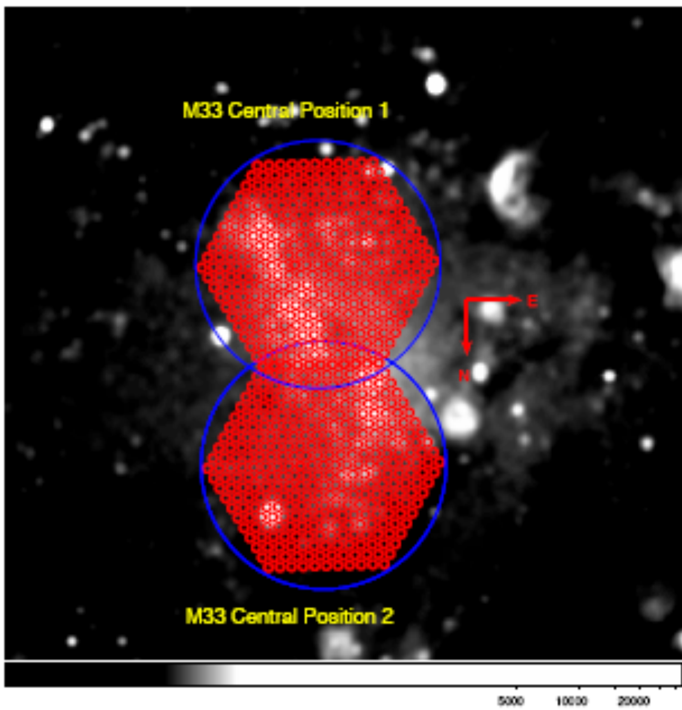

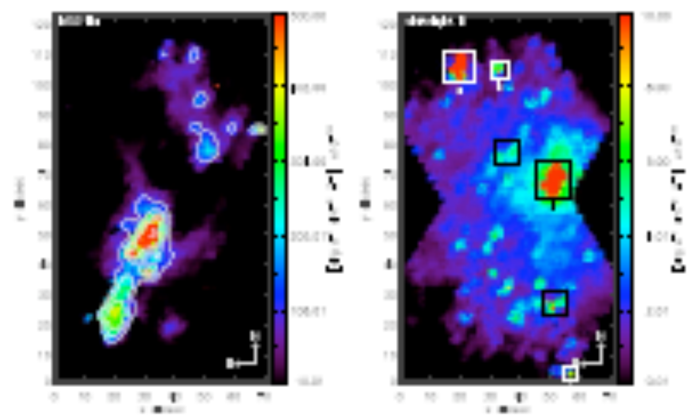

Figure 1: Izquierda: Mapa de la emisión en Hα. Derecha: Mapa de M33 en el cercano infrarrojo (promediado sobre todo el rango espectral.)

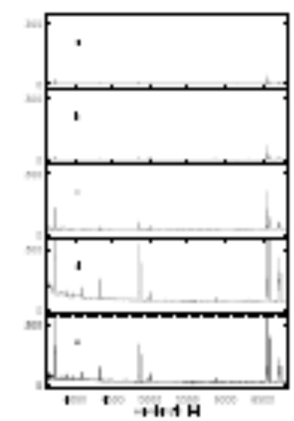

The outer HII region IC 132

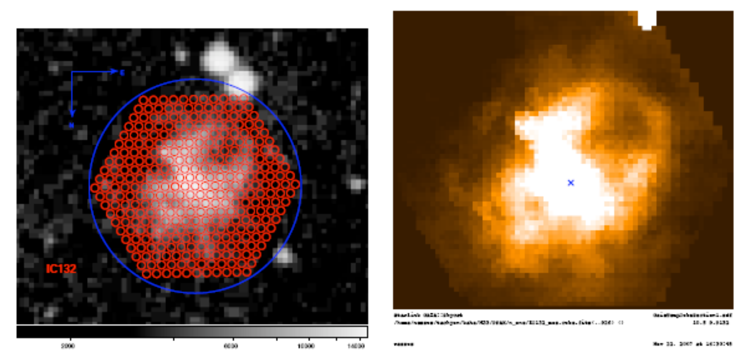

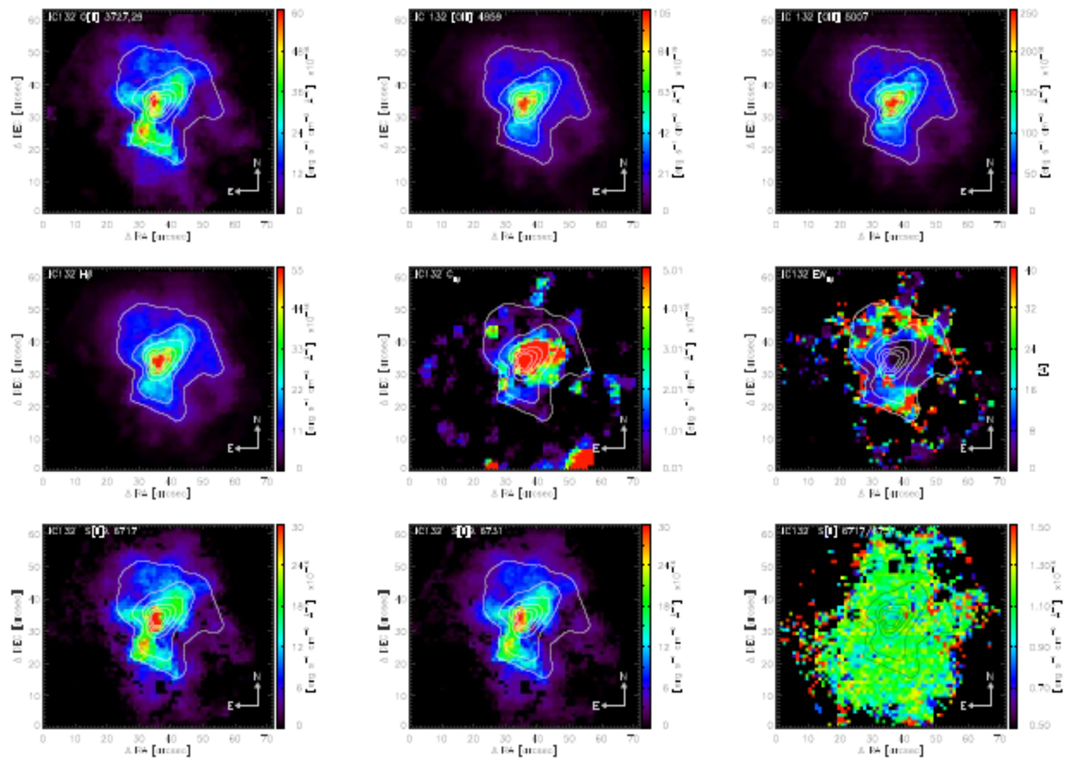

Figure 4: Mapas para IC132. Arriba: [OII]λ 3727,29, [OIII]λ4959 y [OIII]λ 5007 en emisión. En medio: H_β en emisión, continuo en β y EW(H_β). Abajo: [SII]λ 6717 y [SII]λ 6731 en emisión, así como su cociente.

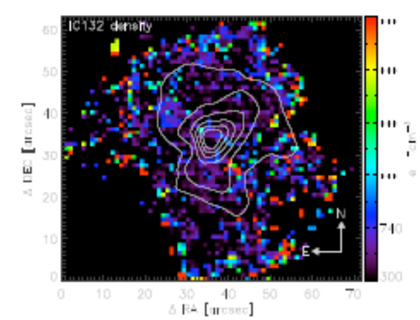

HII regions Geometry & Ionisation structure tests to 3D photo-i models

∃ internal T_e gradients; extinction & dust distribution;
geometrical distribution of massive ionising clusters …

= > **DETAILED IFU STUDY OF NGC 595 IN M 33**

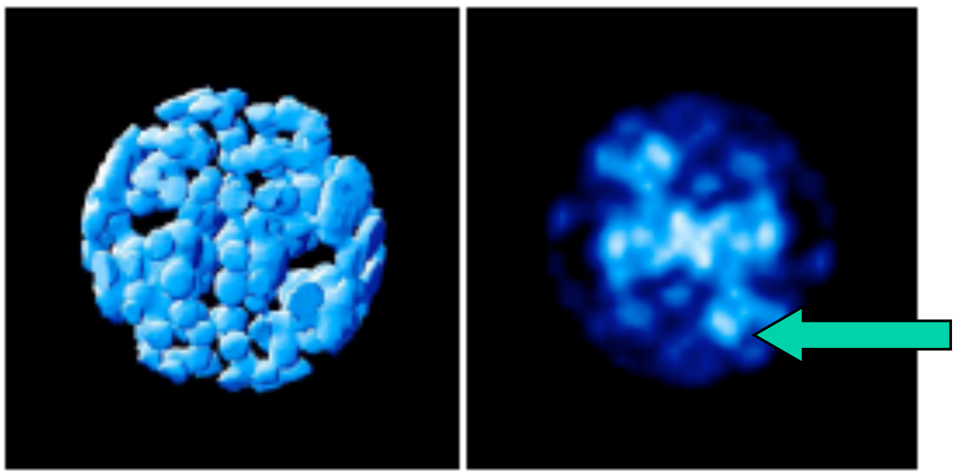

Figure 1. The left panel shows a 3D representation of the Strömgren sphere distribution for case F, plotted as the iso-surfaces where the ionisation fraction of hydrogen is 0.95. The adjacent right panel shows an average projection map of the ionic abundance of H^+.

3D montecarlo photo-ionization models: ionising stars distribution (Ercolano, B. et al. 2007)

Integral Field spectroscopy of the giant HII region NGC 595

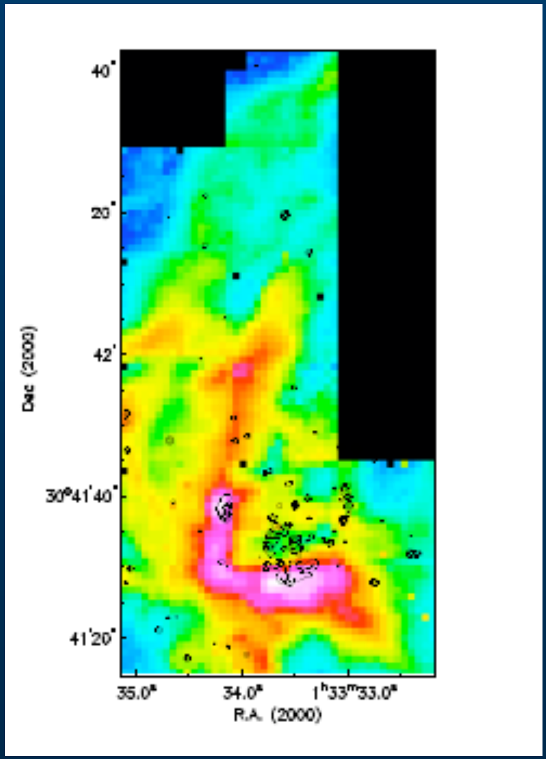

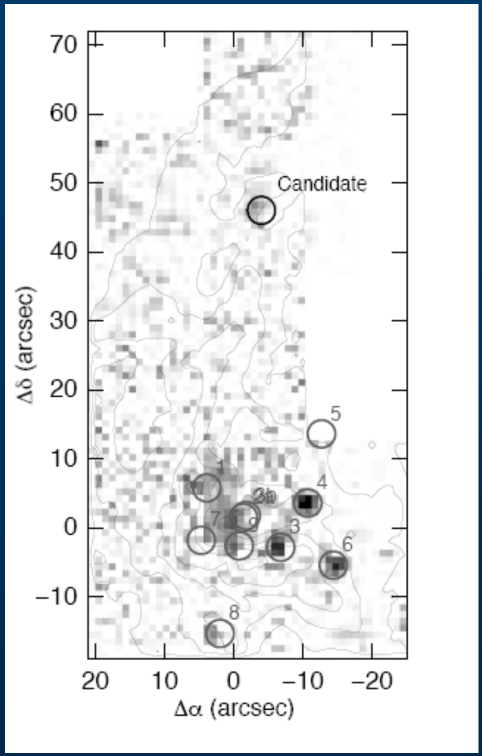

PMAS @ 3.5m Calar Alto
3.4 Å/pix ; 3650 – 6990 Å
47”x 92” ⇔ 174 x 340 pc^2

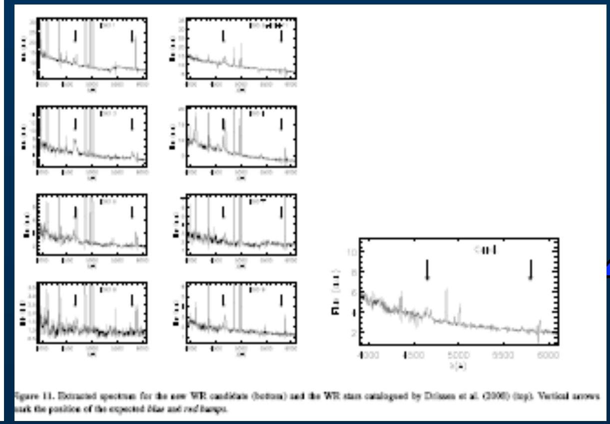

Hα map

Wolf-Rayet stars content

Relaño et al 2009 submitted

M. Relaño, A. Monreal-Ibero, J. M. Vílchez and R. C. Kennicutt

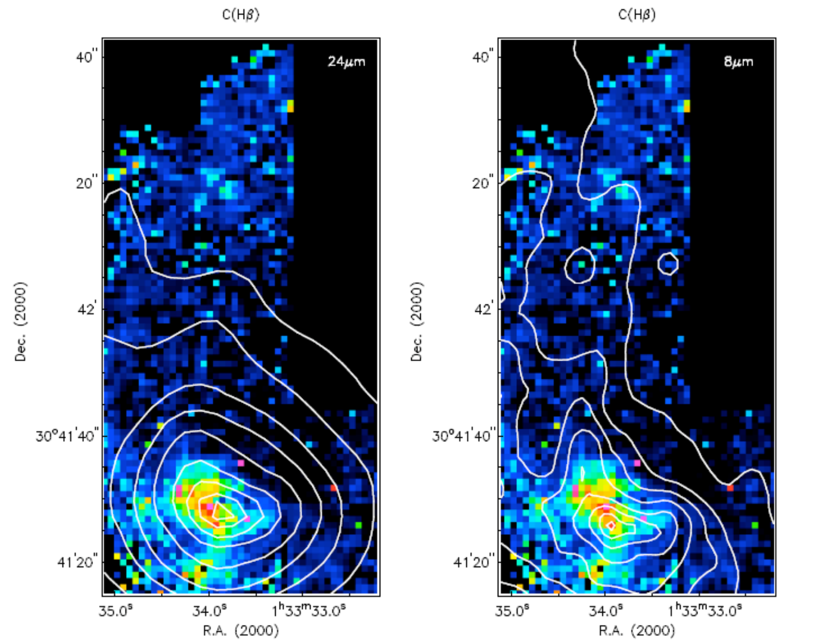

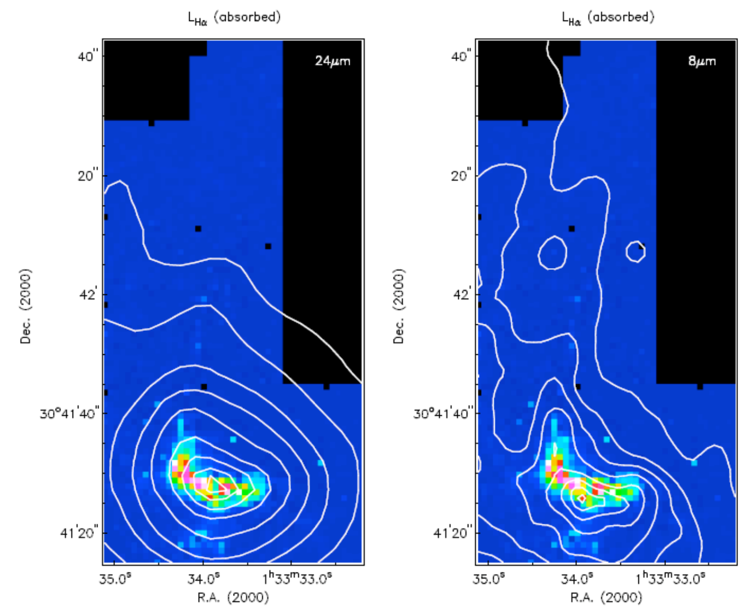

pper: Map of the reddening coefficient C(Hβ) for NGC 595 with 24 μm (left) and 8 μm (right) emission contours overplot. The intensity
the 24 μm and 8 μm emission are at (2, 5, 10, 20, 40, 60, 80, 95)% of the maximum intensity within the region. A 1% contour level
to 3σ and 1σ for the 24 μm and 8 μm emission, respectively. Lower: *Absorbed* Hα luminosity of NGC 595 with 24 μm (left) and
emission contours overplot. The contour levels are the same as in the upper figures.

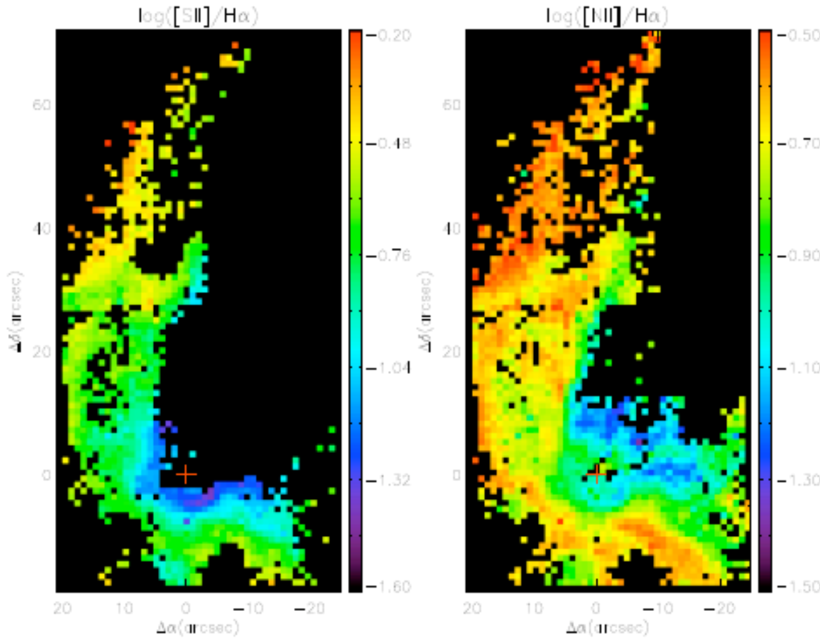

SII/Hα NII/Hα

OIII/Hβ SII6717/6731

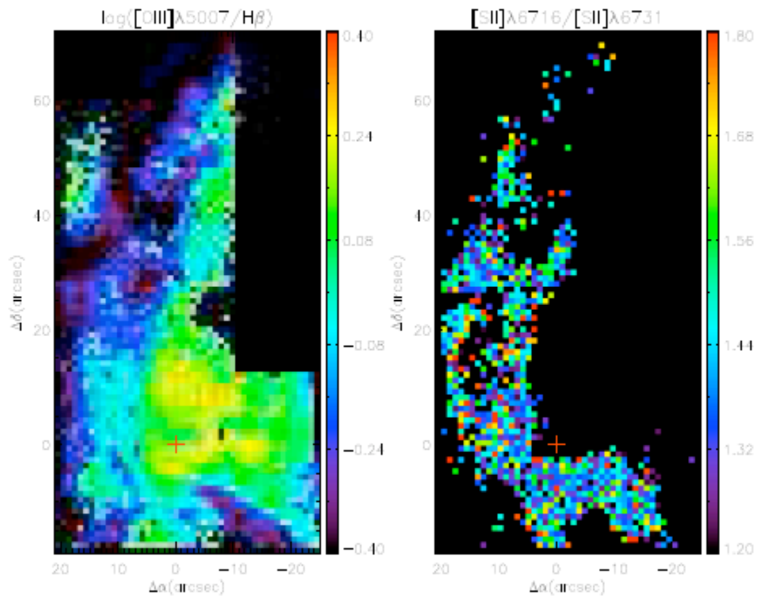

Figure 6. [S ɪɪ]λ6717,31/Hα (upper left), [N ɪɪ]λ6584/Hα (upper right), [O ɪɪɪ]λ5007/Hβ (bottom left) and [S ɪɪ]λ6717/[S ɪɪ]λ6731 (bottom right) emission line ratio maps for the whole face of NGC 595. Only *spaxels* with emission line ratios having relative errors < 30% are shown. Extinction correction for the fitted emission lines was performed in each *spaxel* prior obtaining the emission line ratios shown here. The red cross marks the location of the central and most intense stellar cluster (R.A. (J2000): 1h 33m 33.79s, DEC(J2000): 30d 41m 32.6s) and distances are relative to this position.

OIII/OII

R23

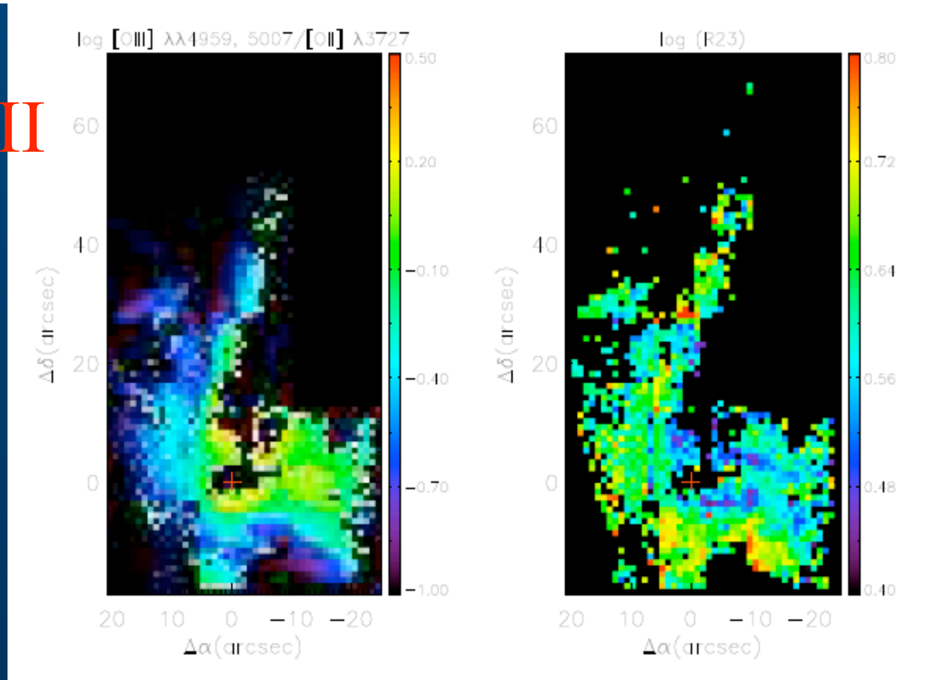

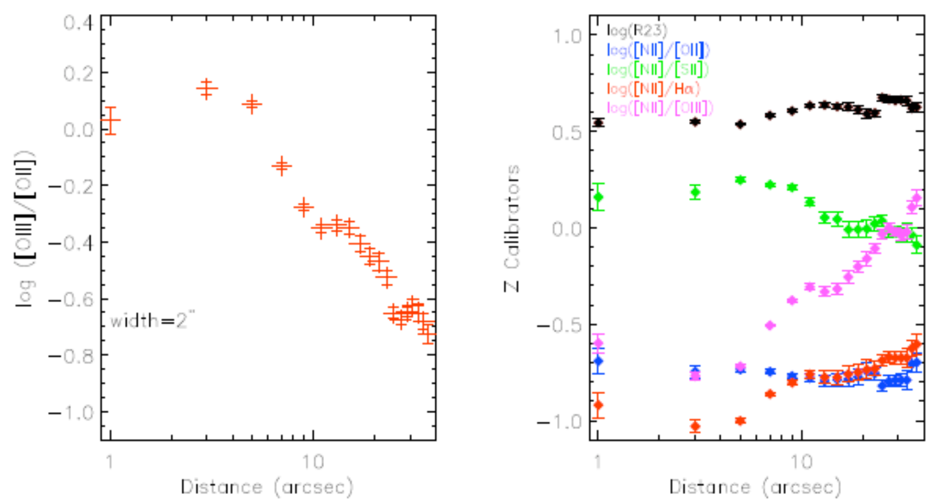

Figure 12. Top: Maps of the oxygen emission line ratios ([O III] λλ4959, 5007/[O II] λ3727) tracing the ionisation parameter (left) and the metallicity (R_{23}= ([O II] λ3727 + [O III] λλ4959,5007)/Hβ) (right). The emission line ratios shown here are those having relative errors $< 30\%$. Bottom: Elliptical radial profiles of [O III]/[O II] (left panel) and R_{23} (right panel, black diamonds). The ellipse parameters are the same as the one used in Figures 5 and 7 and the rings have $2''$ width. In the right panel we also plot radial profile of the main emission line ratios used as metallicity calibrators: [N II]/[O II] (blue), [N II]/[S II] (green), [N II]/Hα (red) and [N II]/[O III] (magenta).

Some open questions

- 2D abundances: IFU maps for M 33
- HII regions, PNs & Massive stars abundances give consistent results => Te fluctuations -> 0
- Theoretical Models calibrations predict abundances (x2 x3) higher than observed
- What is the key physical variable controling massive (ionising) cluster formation across M33 disk?

… …

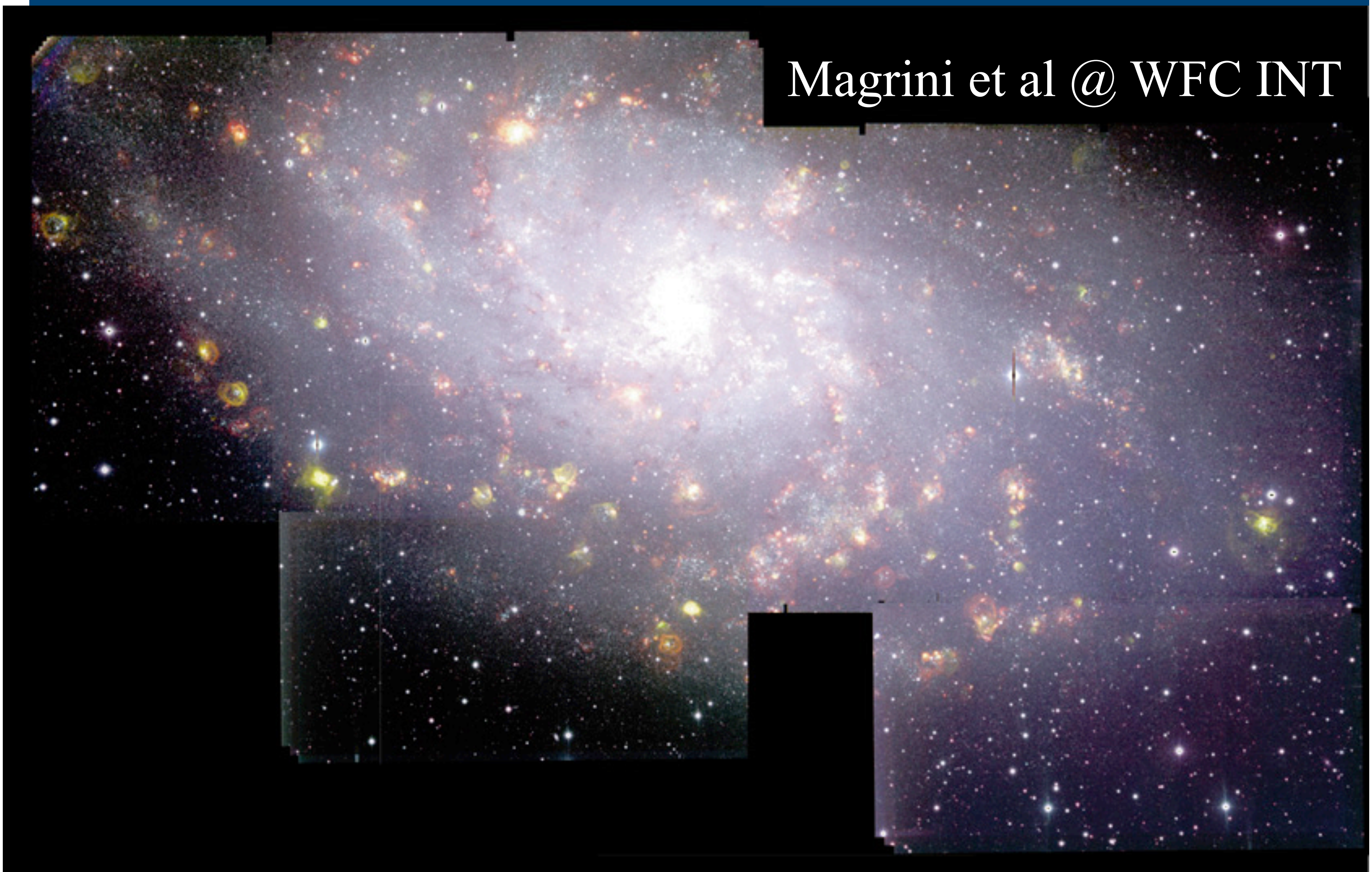
Magrini et al @ WFC INT

Radial abundance gradients: changing their shapes

Shape of radial abundance gradients may be severely affected by **gas dynamical mechanisms, also by presence of bars !** implies caution at the interpretation! =>

2D Abundance gradients needed !!

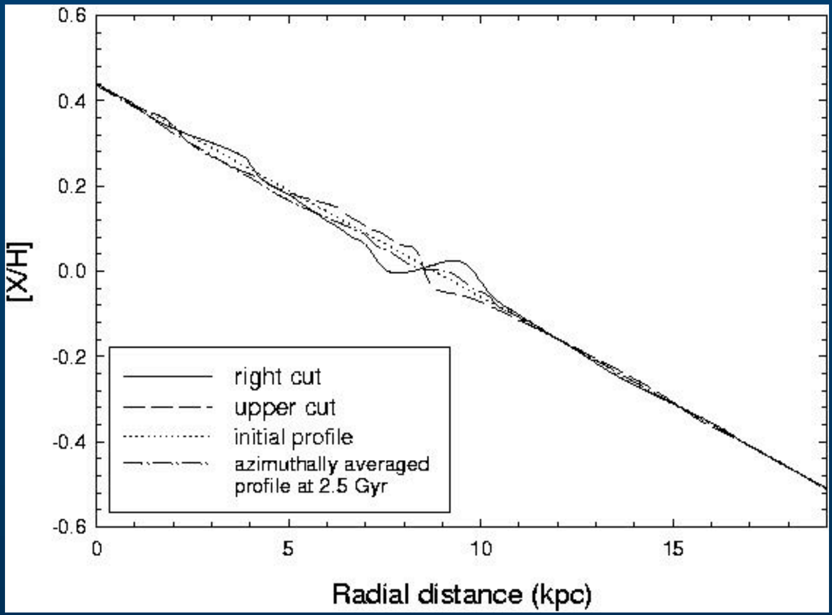

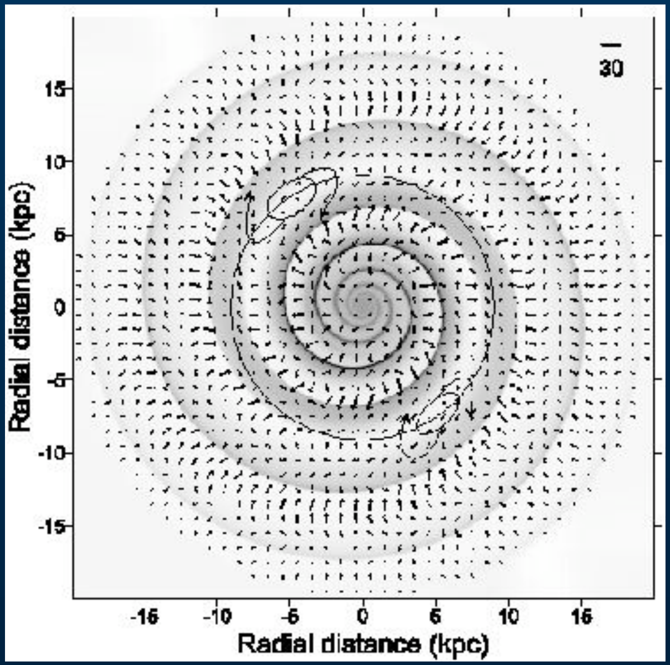

- Radial abundance gradients may be sensible to hydro-dynamical mech. in their disks; ***cyclon/anticyclon gas flows @ co-rotation*** (*Vorobyov 2006 MNRAS 370, 1046);* (also to the presence of a central bar !) .

Abundance Gradients: 1D to 2D

Multi Fibre spec
Optical

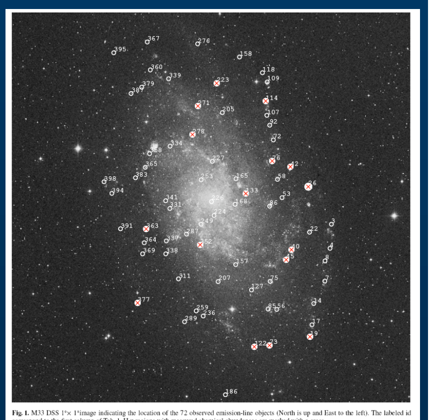

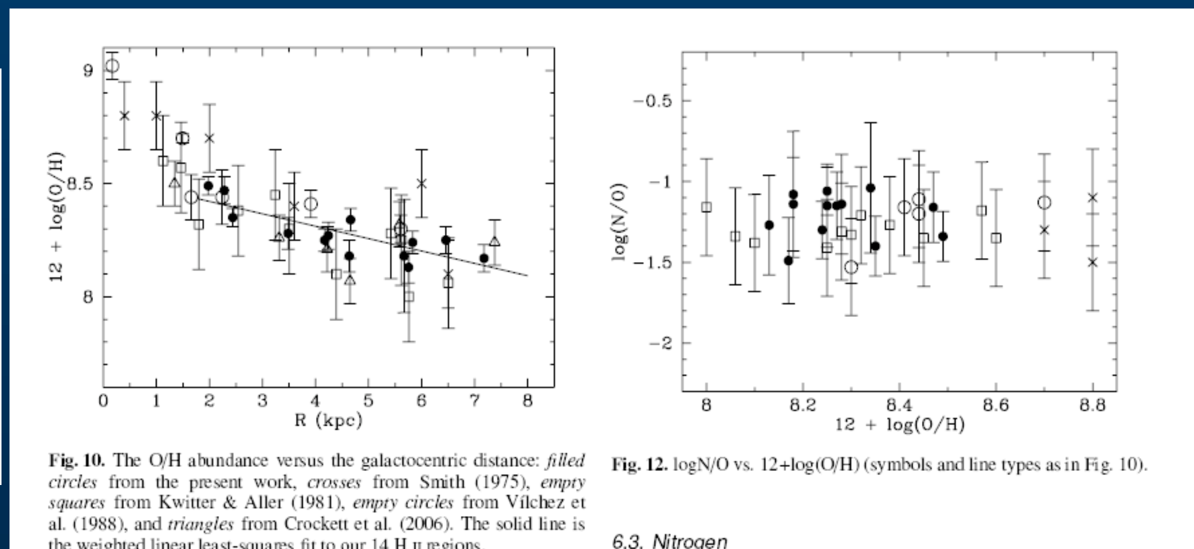

M 33
(Magrini, Vilchez, Mampaso et al 2007)

IMPORTANT!! ***mid Infrared HII regions and optical SG Stars also studied***

M33 Optical and MIR Gradient slopes ***agree ! Also with stellar abundance gradient***

ΔlogO/H/ΔR = 0.054 ± 0.011

(see U, Urbaneja et al 2009; Rubin et al 2008)

M33 => 2D gradients sampling

Oxygen vs. Galactoc. Radius

Rosolowsky & Simon (2007)

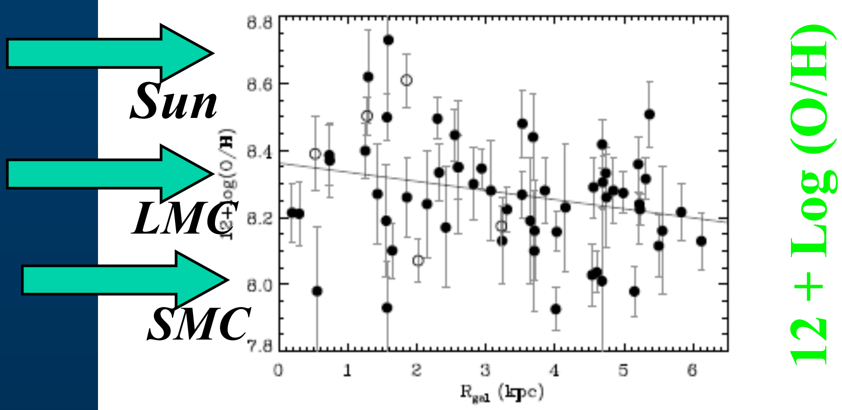

FIG. 2.— Abundances of 61 H II regions in M33 as a function of galactocentric radius. A linear gradient with a slope of −0.027 dex kpc^{-1} is fit to the data (solid line). Regions with significant He II λ4686Å emission are indicated with open symbols.

4 Simon & Rosolowsky

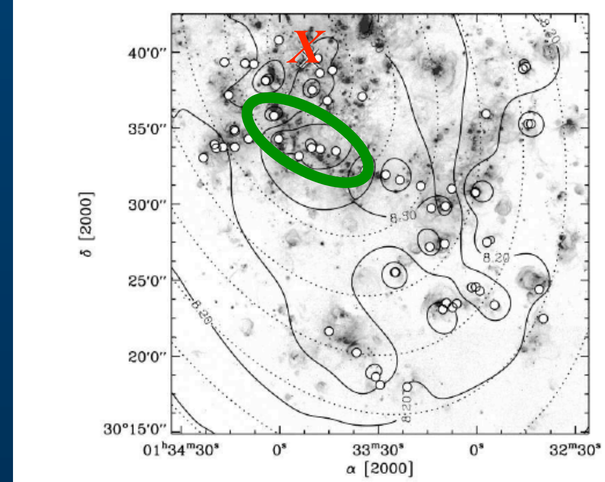

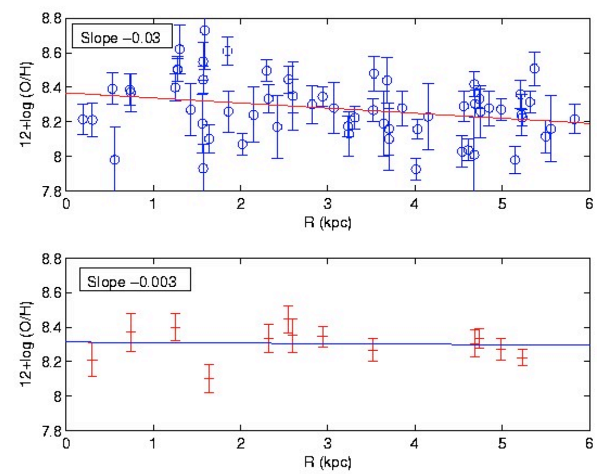

Neon/Oxygen vs. ionization

!!!

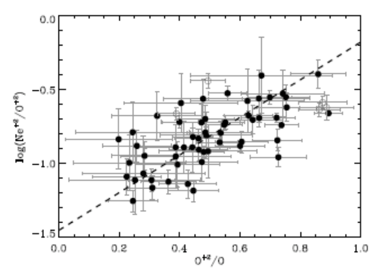

FIG. 4.— Ratio of doubly-ionized neon to doubly-ionized oxygen plotted as a function of O^{+2} ionization fraction. Based on photoionization models, this value should be constant and equal to the Ne/O ratio. However, there is a clear trend of the ratio between the doubly ionized species and the degree of ionization in real H II regions. The dashed line shows the fit given in Equation 2. Regions with significant He II λ4686Å emission are indicated with open symbols.

!!!

Auroral to nebular emission line ratios: current observational limitations

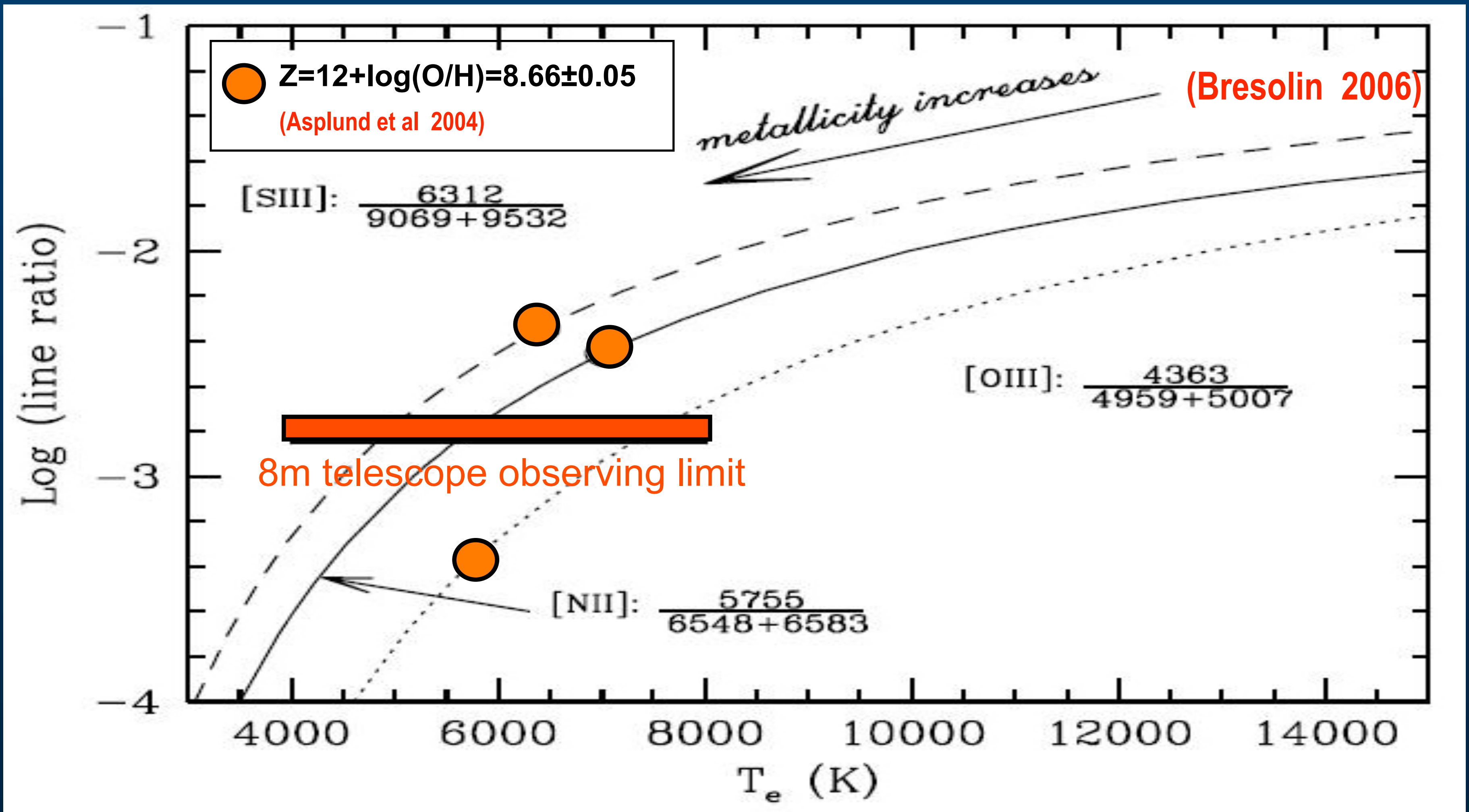

Bright-Line Abundance Calibrations

- Due to the increasing importance of Oxygen as a coolant from 12+log(O/H) ~ 8.2 upwards, the strong-line empirical calibration for O is two-folded.

(Peimbert et al. 2006, Bresolin 2007)

- Sulphur being less abundant than O and its emission lines being at longer λ, its relevance as cooling agents starts at lower temperatures (higher abundances ~ solar).
- → NEW CAL up to 2 x Z_o

O_{23}

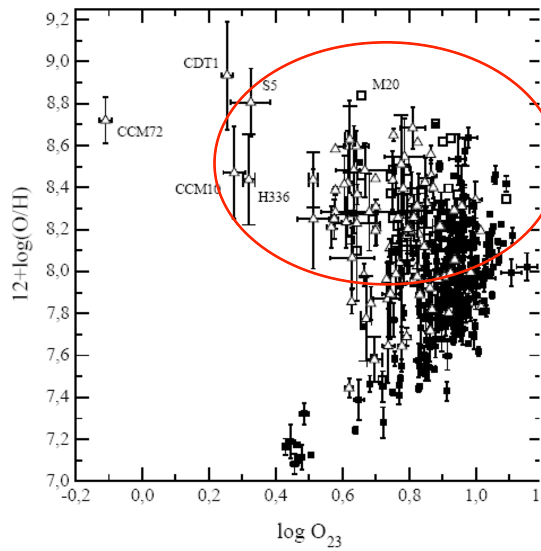

Pérez-Montero & Diaz 2005

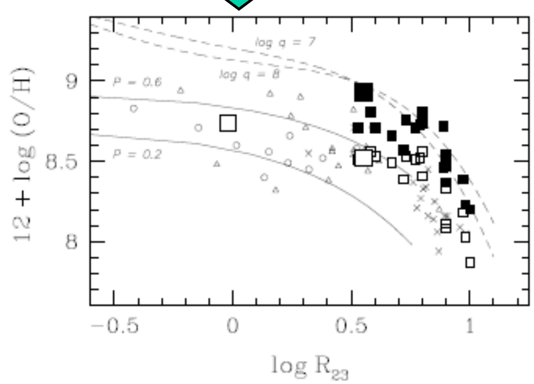

FIG. 6.— The upper, high-metallicity branch of R_{23}. Samples of metal-rich H II regions are taken from KBG03 (crosses) and Bresolin et al. (2004, 2005, open triangles and open circles, respectively). Small squares represent Galactic and extragalactic H II regions, compiled by Peimbert et al. (2006), where abundances have been derived both from collisionally excited lines under the assumption $t^2 = 0$ (open symbols) and from metal recombination lines or an estimate of t^2 (full symbols). The H II regions H493 and H1013 studied in this paper are represented by the large square symbols. The P-method calibration of Pilyugin & Thuan (2005) is shown for $P = 0.2$ and $P = 0.6$ (full lines). The R_{23} calibration based on photoionization models by Kobulnicky & Kewley (2004) is drawn for two values of the ionization parameter, $q = 10^7$ cm s^{-1} (log $U = -3.5$) and $q = 10^8$ cm s^{-1} (log $U = -2.5$) (dashed lines).

S_{23}

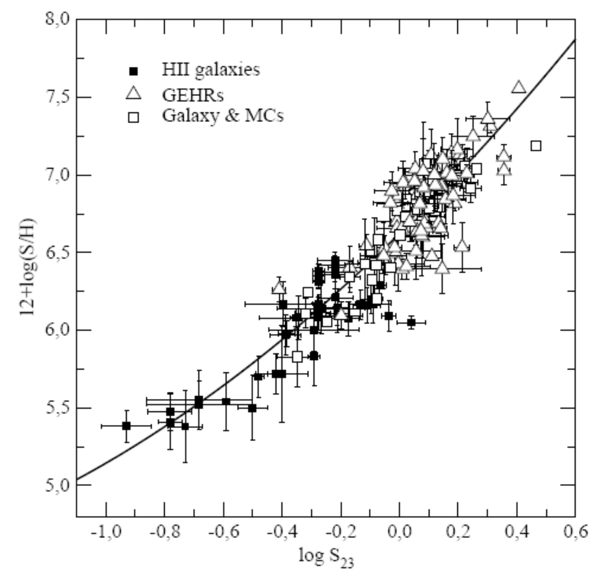

Pérez-Montero, Diaz, Vilchez, & Kehrig 2007

Bright-line calibrations: Z & T_{eff}

R_{23} vs O_{23}

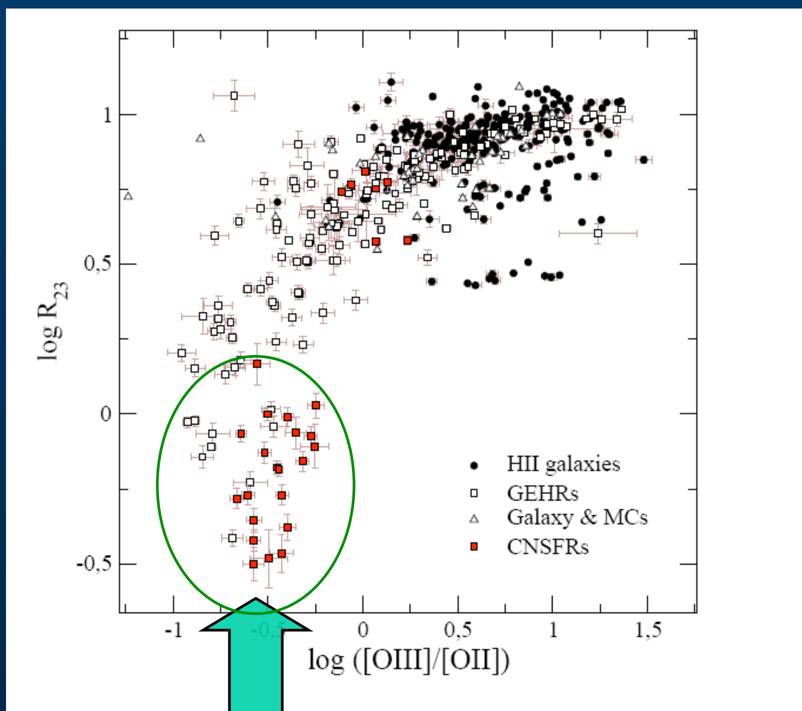

R_{23} vs η'

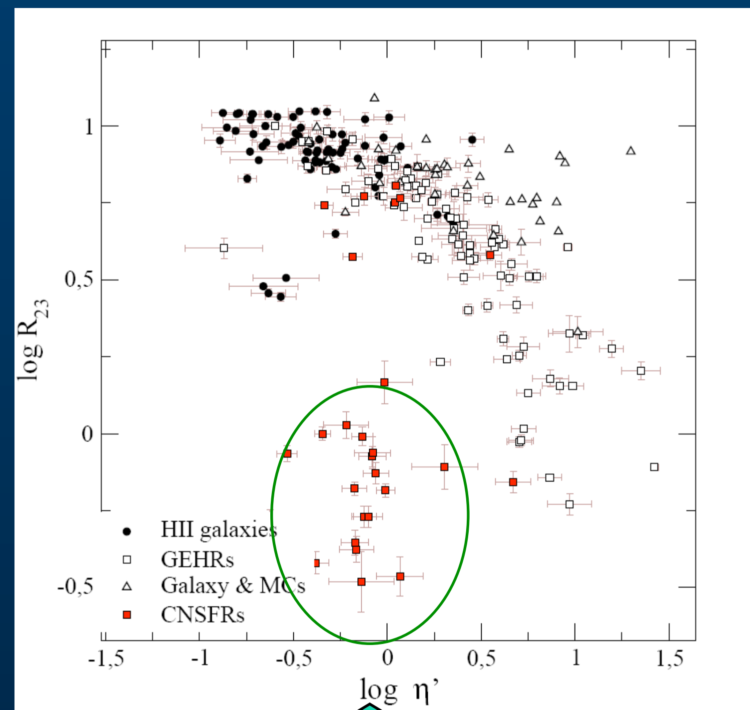

Higher T_{eff} Lower T_{eff}

R_{23}= ([OII]+[OIII])/Hβ

$\eta = [S^{+}/S^{++}]/[O^{+}/O^{++}]$

Softness Parameter (Vilchez & Pagel 1988)

Pérez-Montero, Vilchez et al. in prep.